Contents lists available at SCCE

Journal of Soft Computing in Civil Engineering

Journal homepage: www.jsoftcivil.com

Prediction of Unconfined Compressive Strength of Expansive Soil Amended with Bagasse Ash and Lime Using Artificial Neural Network

D.R. Goutham[1*], A.J. Krishnaiah[2]

1. Research Scholar, Department of Civil Engineering, Malnad College of Engineering, Hassan, India
2. Professor, Department of Civil Engineering, Malnad College of Engineering, Hassan, India

Corresponding author: *goutham.dr03@gmail.com*

https://doi.org/10.22115/SCCE.2023.367214.1545

ARTICLE INFO

Article history:
Received: 25 October 2022
Revised:.14 April 2023
Accepted: 19 May 2023

Keywords:
Bagasse ash;
Lime;
Stabilized expansive soil;
Artificial neural network;
Sensitivity analysis.

ABSTRACT

Expansive soils (ES) have a long history of being difficult to work with in geotechnical engineering. Numerous studies have examined how bagasse ash (BA) and lime affect the unconfined compressive strength (UCS) of ES. Due to the complexities of this composite material, determining the UCS of stabilized ES using traditional methods such as empirical approaches and experimental methods is challenging. The use of artificial neural networks (ANN) for forecasting the UCS of stabilized soil has, however, been the subject of a few studies. This paper presents the results of using rigorous modelling techniques like ANN and multi-variable regression model (MVR) to examine the UCS of BA and a blend of BA-lime (BA + lime) stabilized ES. Laboratory tests were conducted for all dosages of BA and BA-lime admixed ES. 79 samples of data were gathered with various combinations of the experimental variables prepared and used in the construction of ANN and MVR models. The input variables for two models are seven parameters: BA percentage, lime percentage, liquid limit (LL), plastic limit (PL), shrinkage limit (SL), maximum dry density (MDD), and optimum moisture content (OMC), with the output variable being 28-day UCS. The ANN model prediction performance was compared to that of the MVR model. The models were evaluated and contrasted on the training dataset (70% data) and the testing dataset (30% residual data) using the coefficient of determination (R^2), Mean Absolute Error (MAE), and Root Mean Square Error (RMSE) criteria. The findings indicate that the ANN model can predict the UCS of stabilized ES with high accuracy. The relevance of various input factors was estimated via sensitivity analysis utilizing various methodologies. For both the training and testing data sets, the proposed model has an elevated R^2 of 0.9999. It has a minimal MAE and RMSE value of 0.0042 and 0.0217 for training data and 0.0038 and 0.0104 for testing data. As a result, the generated model excels the MVR model in terms of UCS prediction.

How to cite this article: Goutham DR, Krishnaiah AJ. Prediction of unconfined compressive strength of expansive soil amended with bagasse ash and lime using artificial neural network. J Soft Comput Civ Eng 2024;8(1):33-54. https://doi.org/10.22115/scce.2023.367214.1545

1. Introduction

Soil stabilization is a technique for enhancing the behaviour of soil under applied stresses. Recently, a variety of soil improvement approaches, classified as mechanical and chemical, have been applied. The most prevalent mechanical method for improving expansive soil deposits is soil reinforcement. Chemical supplements are also employed as an enhancement approach [1]. Due to their efficiency in lowering expansive qualities, boosting strength, lowering the plasticity index, limiting the possibility for swell and shrinkage, and regulating volume change, lime and cement are frequently employed in chemical treatments of cohesive soils with expansive properties [2]. Bagasse ash is a waste product that is normally disposed of in pits but is also utilized as a soil amendment in some regions due to its high pozzolona content [3].

The review of the literature finds that there has been minimal study on soil stabilization by BA and lime. In recent years, the use of BA and lime in expansive soil has attracted the attention of soil scientists. Researchers examined the effects of BA and lime on improving the properties of clayey soil. The study conducted by Osinubi et al., [4] concentrated on the impact of BA from 0 to 12% at 2% intervals by weight of dry soil on the geotechnical characteristics of the weak lateritic soil. Lateritic soil treated with 2% bagasse ash exhibited peak 7-day UCS and California Bearing Ratio (CBR) readings of 836 kN/m^2 and 16%. Nethravathi et al., [5] investigated on the impact of BA and lime on the ES. The BA ranges from 10 to 60% at 10% intervals by dry soil weight, while the lime ranges from 1 to 5% at 1% intervals by dry soil weight. The strength has been increased to the optimum BA dosage of 20%. When 20% BA and 4% lime were added to the soil, the strength improved even more for different curing intervals. Similar work has been reported by Dang et al., [6] conducted a study to explore the effects of bagasse fibres on the engineering properties of ES, 0.5%, 1.0%, and 2.0% randomly oriented bagasse material was added to ES, and hydrated lime-ES combined with varied bagasse fibre fractions was also tested. The results of this test indicate that bagasse fibre reinforcement combined with hydrated lime enhanced the compressive strength of ES, as curing period and supplement amount enhanced. James et al., [7] perfomed a work on stabilization procedure supplemented with 3% lime and various concentrations of BA (viz., 0.25%, 0.5%, 1%, and 2%) and coconut shell powder (CSP) individually was performed, and the effectiveness of the amendment on the UCS, plasticity, and swell-shrinkage of the ES was evaluated. According to the study's findings, BA modification of lime stabilization worked better than CSP in terms of enhancing UCS, plasticity, and swell-shrink. Reddy et al., [8] studied on black cotton soil (BCS) blended with lime in varying concentrations of 2%, 4%, and 6%. According to soaked CBR studies on BCS, 4% lime concentration is considered optimal. The inclusion of 4% lime in BCS for stabilization did not produce the requisite result of CBR for subbase. As a consequence, brick powder is supplied in the range of 20 to 80% at 20% increments by dry weight of soil. As compared to 4% lime-stabilized soil, a 20% brick powder combination increased the soaked CBR value by roughly 135%. The literatures mentioned above supports the argument that adding BA and lime to ES increases its strength. The investigations by other researchers [9–11] reported the same outcomes. An accurate model to forecast the strength of BA-lime treated soils is required due to the remarkable growth in the usage of BA and lime to enhance cohesive soils and their successful implementation in earlier research.

Alavi et al. [12] worked on the use of ANN to forecast the MDD and OMC of a soil-stabilizer combination was investigated in this study. Five ANN models are built, utilizing various input variable pairs. A parametric analysis was also carried out to assess the adaptability of MDD and OMC to changes in the most influential input factors. The findings show that the suggested models reliability is good in contrast to the data from experiments. Mozumder et al. [13] have studied on the materials such as ground granulated blast furnace slag (GGBS), fly ash (FA), and a mixture of GGBS and FA. With varied combinations of the test factors, a 28-day UCS of 283 stabilized samples was obtained. Additionally, a neural interpreting diagram (NID) to visualize the influence of input factors on UCS is illustrated. Salahudeen et al. [14] carried out a research on ANN as a soft computing technique, trained with the feed-forward back-propagation technique, to simulate the OMC and MDD of cement kiln dust-stabilized BCS. All of the simulated findings are favourable, and there was a significant agreement between the actual OMC and MDD values acquired from testing in the laboratory and the anticipated values obtained using ANN. Bahmed et al. [15] have construct three models based on ANNs that forecast all of the plasticity index (PI), OMC, and MDD values of subgrade soil improved with lime using fundamental soil data that are always accessible to engineers. Three distinct models are established, each pertaining to the optimal architecture for the three attributes, and each of them may be used as a reliable method to forecast the PI, OMC, and MDD of lime-stabilized ES. Nazeer and Dutta [16] carried out research that employs machine learning approaches to estimate the bearing capacity formula of an E-shaped foundation exposed to a vertical concentric force and positioned on layered sand. The data used in the computation was taken from the finite element modelling of a similar footing. Two models have been developed, and both of them were shown to be capable of predicting the bearing capacity of the E-shaped foundation with sufficient precision. Dutta et al. [17] report their work on the free swell index of ES using an ANN. The ANN model's input variables were the PI and shrinkage index, while its outcome was the free swell index (FSI). The study discovered that, after implementing an ANN model, the forecasting accuracy of the FSI of ES was fairly excellent. Soft computing techniques have been effectively used in the past several decades as a robust tool to solve and evaluate a variety of geotechnical engineering challenges [18,19]. The issues relating to soil deposition are typically quite complicated. Additionally, a variety of factors determine how soils stabilized with chemical additions behave.

The current research aims to stabilize clayey soil using BA and lime. The source ingredients such as BA and a mixture of BA + lime were also included in the current study to assess the stabilization effect among them, and the test findings were reported using a 28-day UCS value. An ANN-based UCS prediction model was developed for optimal and effective stabilization. The suggested ANN model's prediction effectiveness was contrasted to that of the MVR model. The influence of various input factors on the predicted UCS of stabilized specimens was investigated and measured using sensitivity analysis. The prediction model was developed to predict the UCS value of a BA-lime stabilized ES and will be helpful for researchers and geotechnical engineers in determining the strength capacity of the soil. Traditional experimental approaches are labour and time intensive in determining the UCS. The predictive model can also be used to calculate the ideal amounts of BA and lime to deploy in an ES with known Atterberg's limits and compaction properties.

2. Methods

2.1. Experimental data

The expansive soil utilized in the investigations was obtained at a depth of 1.5 m below ground in Kadur, Chikkamagaluru district, India. To ensure that the BA was mixed equally, the soil was pulverised (to a size smaller than 4.75 mm) using a hammer and then sundried to reduce the moisture content to around 0%. The engineering features of air-dried expansive soil as determined experimentally using conventional test approaches are summarised in Table 1. According to grain size analysis IS 2720 [20], 61.2% of the particles are clay size and 20.8% are silt size. The soil is classified as highly compressible clay, CH according to IS 1498 [21]. The lime utilized in the study was laboratory grade hydrated lime produced by Nandi. BA was obtained from Mugulavalli Sugar Mills Pvt. Ltd. in the Karnataka city of Chikkamagaluru, India. The chemical content of the compounds used in the investigation is listed in Table 2.

Table 1
Soil classification and properties of ES.

Sl. No.	Property of soil	Values
1.	Specific gravity	2.63
2.	Fine sand fraction (%)	18.0
3.	Silt fraction (%)	20.8
4.	Clay fraction (%)	61.2
5.	Liquid Limit (%)	65
6.	Plastic Limit (%)	27
7.	Plasticity index (%)	38
8.	Shrinkage Limit (%)	13
9.	Optimum Moisture Content (%)	28
10.	Dry Density (kN/m^3)	13.3
11.	Free swell index (%)	97
12.	Soil Classification	CH
13.	UCS (kPa)	51.12

Table 2
Chemical composition of ES, lime, and BA.

Type of Material	SiO_2 (%)	Al_2O_3 (%)	CaO (%)	Fe_2O_3 (%)	K_2O (%)	MgO (%)	MnO (%)	Na_2O (%)	P_2O_5 (%)	TiO_2 (%)	SO_3 (%)
ES	64.71	17.12	2.40	7.89	2.15	1.68	0.03	1.53	0.03	0.99	0.30
Lime	0.22	0.06	72.09	0.05	0.004	15.30	0.003	0.06	0.005	0.004	0.03
BA	63.92	5.340	12.10	4.28	3.85	0.91	0.03	1.02	1.10	0.03	0.05

As shown in Table 2, Energy Dispersive X-Ray investigation was also employed in this experiment to examine the stability of expanding soil as well as its chemical composition and constituent parts. The three main substances, which together make up around 84% of expansive soil, are SiO_2, Al_2O_3, and Fe_2O_3. As a consequence, it is feasible to draw the conclusion that quartz mineral concentration in coarse mineral and aluminium silicate clay mineral amplification in fine mineral. According to ASTM D 653-03 [22], natural pozzolans are categorised as class-F pozzolans if the ratio of SiO_2, Al_2O_3, and Fe_2O_3 to the overall mass is more than 70%. As a result, the BA employed in the present research is a pozzolan of class F.

The ES was weighed to the closest gramme and oven dried for 24 hours at 110 ± 5°C before being rigorously combined with the source materials in an appliance until a homogeneous blend was achieved. The quantity of stabilizers varies as a percentage of the dry weight of soil solids, ranging from 0 to 18% for BA and 0 to 6% for lime. With varying dosages of BA and lime, tests such as liquid limit [23], plastic limit [23], shrinkage limit [24], maximum dry density [25], optimum moisture content [25], and UCS [26] were performed. The Table 3 shows the test results of all the 79 samples of experimental findings. Fig. 1 shows the results of unconfined compressive strength.

The choice of BA content ranging from 0 to 18% at an interval of 3% in the soil was made from the past research work carried out for the expansive soil. The pH test yielded a result of 3.5% for the minimal lime level necessary for current ES stabilization. Using UCS testing, the ideal lime concentration was found to be 4.5%. Therefore, the lime content has been varied from 0 to 6% at an interval of 0.5% with different percentages of BA content to understand the combined effect on the UCS test results.

Table 3
Experimental test results.

Sample No.	BA (%)	Lime (%)	LL (%)	PL (%)	SL (%)	MDD (kN/m^3)	OMC (%)	UCS (kPa)	Remark
1.	0	0	65	27	13	13.3	28	51.12	Training
2.	3	0	58	30	13	12.5	28.5	78.68	Training
3.	6	0	56	35	15	11.8	29.5	92.23	Training
4.	9	0	54.5	37	16	11.5	30	109.25	Test
5.	12	0	52	39	18	11	31	132	Training
6.	15	0	51	39.5	21	10.7	32	112.58	Training
7.	18	0	50	40	22	10.5	33	91.5	Training
8.	3	0.5	57.61	29.61	12.61	12.11	28.11	78.29	Training
9.	6	0.5	55.99	34.99	14.99	11.79	29.49	92.22	Test
10.	9	0.5	54.68	37.18	16.18	11.68	30.18	109.43	Training
11.	12	0.5	52.77	39.77	18.77	11.77	31.77	132.77	Training
12.	15	0.5	51.37	39.87	21.37	11.07	32.37	112.95	Training
13.	18	0.5	49.61	39.61	21.61	10.11	32.61	91.11	Training
14.	3	1.0	57.23	29.23	12.23	11.73	27.73	77.91	Test
15.	6	1.0	55.97	34.97	14.97	11.77	29.47	92.2	Training
16.	9	1.0	54.86	37.36	16.36	11.86	30.36	109.61	Training
17.	12	1.0	53.54	40.54	19.54	12.54	32.54	133.54	Test
18.	15	1.0	51.74	40.24	21.74	11.44	32.74	113.32	Training
19.	18	1.0	49.21	39.21	21.21	9.71	32.21	90.71	Test
20.	3	1.5	56.84	28.84	11.84	11.34	27.34	77.52	Training
21.	6	1.5	55.96	34.96	14.96	11.76	29.46	92.19	Training
22.	9	1.5	55.03	37.53	16.53	12.03	30.53	109.78	Training
23.	12	1.5	54.31	41.31	20.31	13.31	33.31	134.31	Test
24.	15	1.5	52.11	40.61	22.11	11.81	33.11	113.69	Training
25.	18	1.5	48.82	38.82	20.82	9.32	31.82	90.32	Test
26.	3	2.0	61.7	31.1	22.9	12.4	29.8	68.55	Test
27.	6	2.0	60.7	38.1	27.9	11.8	30.8	82.35	Training
28.	9	2.0	59.2	42.1	31.9	11.5	32.3	148.37	Training
29.	12	2.0	57.7	46.1	35.9	10.9	33.8	183.62	Training

30.	15	2.0	55.7	51.1	40.9	10.6	34.8	276.32	Test
31.	18	2.0	55.7	53.1	44.9	10.4	36.3	209.32	Training
32.	3	2.5	59.77	29.17	20.97	10.47	27.87	66.62	Training
33.	6	2.5	60.63	38.03	27.83	11.73	30.73	82.28	Training
34.	9	2.5	60.09	42.99	32.79	12.39	33.19	149.26	Training
35.	12	2.5	61.54	49.94	39.74	14.74	37.64	187.46	Training
36.	15	2.5	57.56	52.96	42.76	12.46	36.66	278.18	Test
37.	18	2.5	53.73	51.13	42.93	8.43	34.33	207.35	Training
38.	3	3.0	59.39	28.79	20.59	10.09	27.49	66.24	Training
39.	6	3.0	60.61	38.01	27.81	11.71	30.71	82.26	Training
40.	9	3.0	60.27	43.17	32.97	12.57	33.37	149.44	Test
41.	12	3.0	62.31	50.71	40.51	15.51	38.41	188.23	Training
42.	15	3.0	57.93	53.33	43.13	12.83	37.03	278.55	Training
43.	18	3.0	53.33	50.73	42.53	8.03	33.93	206.95	Training
44.	3	3.5	59	28.4	20.2	9.7	27.1	65.85	Training
45.	6	3.5	60.6	38	27.8	11.7	30.7	82.25	Test
46.	9	3.5	60.45	43.35	33.15	12.75	33.55	149.62	Training
47.	12	3.5	63.08	51.48	41.28	16.28	39.18	189	Training
48.	15	3.5	58.3	53.7	43.5	13.2	37.4	278.92	Training
49.	18	3.5	52.94	50.34	42.14	7.64	33.54	206.56	Training
50.	3	4.0	63	32	24	12.7	30	74.25	Test
51.	6	4.0	62	39	29	12.1	31	88.05	Test
52.	9	4.0	60.5	43	33	11.8	32.5	154.07	Training
53.	12	4.0	59	47	37	11.2	34	189.32	Training
54.	15	4.0	57	52	42	10.9	35	282.02	Training
55.	18	4.0	57	54	46	10.7	36.5	215.02	Training
56.	3	4.5	59.53	28.53	20.53	9.23	26.53	70.78	Training
57.	6	4.5	61.87	38.87	28.87	11.97	30.87	87.92	Test
58.	9	4.5	62.1	44.6	34.6	13.4	34.1	155.67	Training
59.	12	4.5	65.92	53.92	43.92	18.12	40.92	196.24	Test
60.	15	4.5	60.34	55.34	45.34	14.24	38.34	285.36	Test
61.	18	4.5	53.45	50.45	42.45	7.15	32.95	211.47	Training
62.	3	5.0	59.14	28.14	20.14	8.84	26.14	70.39	Training
63.	6	5.0	61.86	38.86	28.86	11.96	30.86	87.91	Training
64.	9	5.0	62.28	44.78	34.78	13.58	34.28	155.85	Test
65.	12	5.0	66.69	54.69	44.69	18.89	41.69	197.01	Test
66.	15	5.0	60.71	55.71	45.71	14.61	38.71	285.73	Training
67.	18	5.0	53.05	50.05	42.05	6.75	32.55	211.07	Training
68.	3	5.5	58.76	27.76	19.76	8.46	25.76	70.01	Training
69.	6	5.5	61.84	38.84	28.84	11.94	30.84	87.89	Test
70.	9	5.5	62.46	44.96	34.96	13.76	34.46	156.03	Test
71.	12	5.5	67.45	55.45	45.45	19.65	42.45	197.77	Training
72.	15	5.5	61.08	56.08	46.08	14.98	39.08	286.1	Training
73.	18	5.5	52.66	49.66	41.66	6.36	32.16	210.68	Training
74.	3	6.0	65.1	34.04	25.83	14.838	29.667	138.84	Test
75.	6	6.0	64.1	41.04	30.83	14.238	30.667	164.65	Test
76.	9	6.0	62.6	45.04	34.83	13.938	32.167	288.11	Test
77.	12	6.0	61.1	49.04	38.83	13.338	33.667	354.02	Training
78.	15	6.0	59.1	54.04	43.83	13.038	34.667	527.37	Training
79.	18	6.0	59.1	56.04	47.83	12.838	36.167	402.08	Training

The UCS specimens were produced in a 38 mm x 76 mm fixed volume split mould. Defined amounts of soil, lime, and BA were placed in a pan and blended by hand in dry circumstances to reach the desired dry density. The specimens were right away sealed within a polythene cover so they could cure. Each of the combinations was tested on three specimens. To determine the strength of the stabilized soil, the specimens were allowed to cure at 28 ± 2°C for periods of 28 days. The specimens were taken out of their sealed polythene wraps after the designated curing times and loaded until they fractured at a strain rate of 0.625 mm/min.

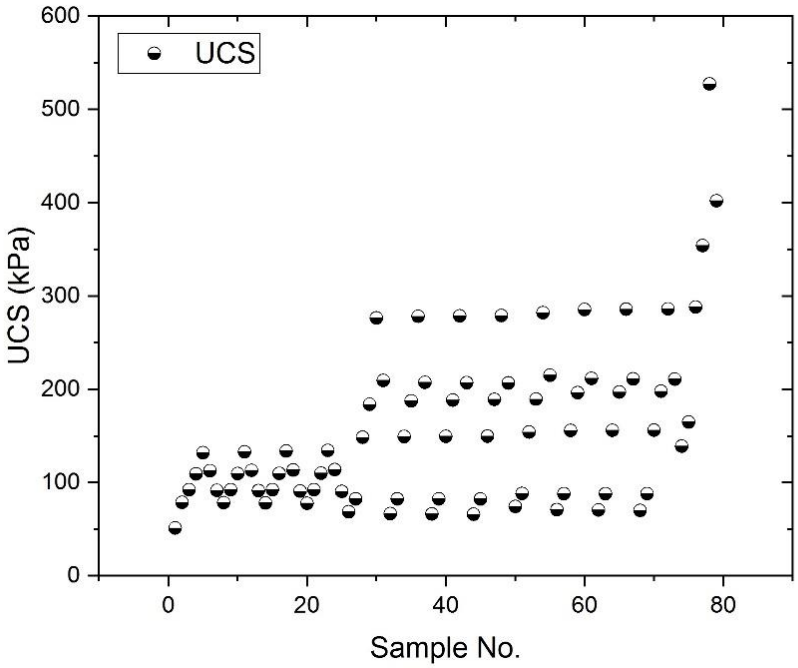

Fig. 1. Collected laboratory data of stabilized ES specimens.

2.2. ANN model development

Numerous geotechnical engineering issues have been solved with ANN in the past. Due to this, and since it is possible to get more information in the literature, the present study refrains from describing ANN in detail [27,28].

A total of 79 samples of experimental findings of 28 day UCS of ES stabilized with BA and lime were collected for this investigation. BA-admixed cohesive soils and BA-lime combinations were used in the experiments. A predictive ANN model based on neural network technique was established. Input parameters for the ANN include the liquid limit (LL), plastic limit (PL), shrinkage limit (SL), percentage of BA (%), percentage of lime (%), MDD (kN/m^3), and OMC (%). These input parameters have certain levels of effect on the UCS values of the ES soil. The change in these parameters will affect the end results. The output parameter is the 28-day UCS in kPa. With the help of the neural network toolkit, ANN modelling was implemented in the MATLAB R2014a environment. The recommended data split of the ANN model is used to obtain statistically constant training and testing data [28]. 30% of the experimental data was used to test the trained model, while the remaining 70% was used to train the model. Table 4 lists the statistical characteristics of the training and testing data. There is no set rule for determining the

number of concealed layers and nodes. Fig. 2 illustrates the flow path for developing a good ANN model.

The model was created by combining the best mapping scheme, the back propagation network, and the Levengberg-Maquardt method for training, resulting in the quickest training technique for multilayer perceptron, the most common class of ANN that employ the feed-forward architecture [15]. Fig. 3 shows the architecture of the current ANN model for UCS prediction. After multiple trial and error procedures, the optimal performance was discovered to be seven hidden neurons in a single hidden layer, and this judgement was based on the value of squared regression and mean squared error (MSE). The output parameter UCS is represented by a single neuron.

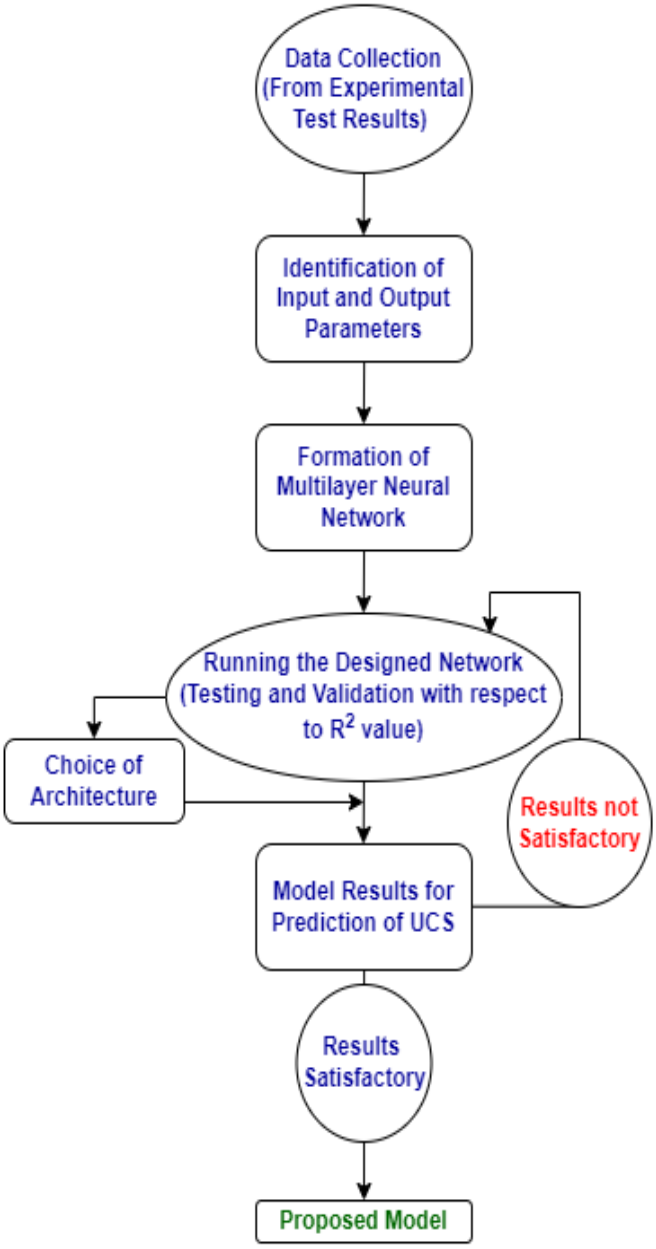

Fig. 2. ANN flow pattern.

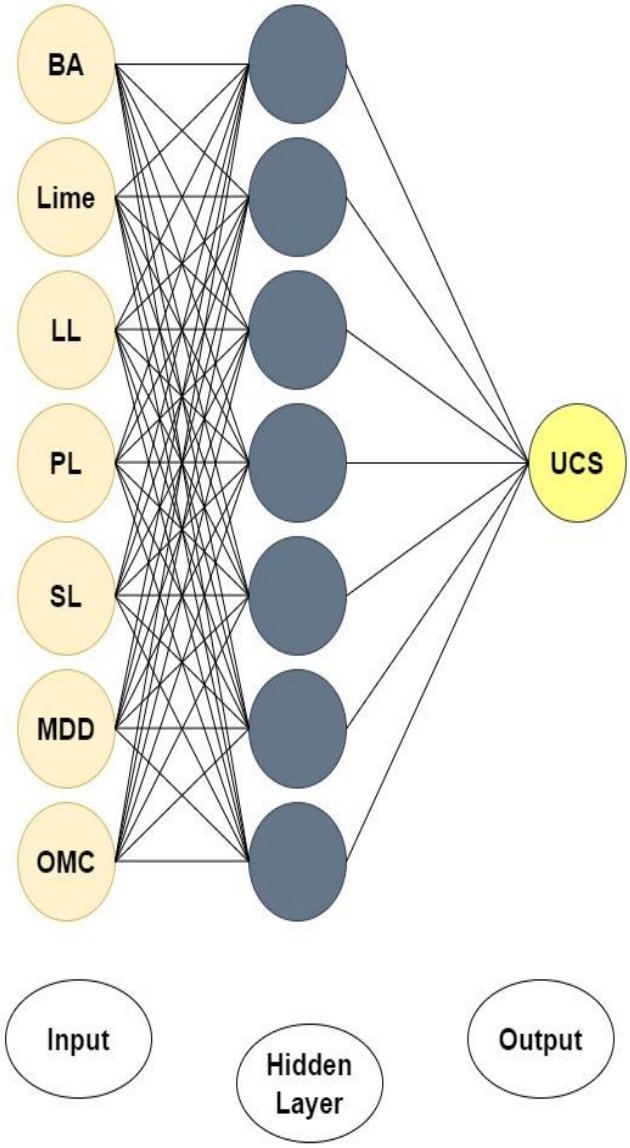

Fig. 3. The ANN model's framework for UCS prediction.

The efficacy of the ANN model was assessed using three statistical metrics: the root mean squared error (RMSE), mean absolute error (MAE), and coefficient of determination (R^2) were computed using equations 1, 2 and 3. Table 5 depicts training parameters used in developing a ANN model.

$$R^2 = \frac{\sum_N (Y_m)^2 - \sum_N (Y_m - Y_p)^2}{\sum_N (Y_m)^2} \quad (1)$$

$$MAE = \frac{\sum_N |Y_m - Y_P|}{N} \quad (2)$$

$$RMSE = \sqrt{\frac{\sum_N (Y_m - Y_p)^2}{N}} \quad (3)$$

where Y_m is experimentally determined values, Y_P is estimated values by ANN model, and the N represents the number of laboratory measurements.

Table 4
Analysis of laboratory data using statistics for model construction.

Input Parameter	All data				Training set				Testing set			
	Min	Max	Mean	SD	Min	Max	Mean	SD	Min	Max	Mean	SD
BA	0	18	10.36	5.22	6	18	10.85	5.41	3	18	9.25	4.57
Lime	0	6	2.96	1.88	0	6	2.8	1.85	0	6	3.33	1.91
LL	48.82	67.45	58.06	4.30	49.61	67.45	57.44	3.91	48.82	66.69	59.48	4.79
PL	27	56.08	42.16	8.49	27	56.08	42.38	8.93	29.23	55.34	41.66	7.34
SL	11.84	47.83	29.68	11.02	11.84	47.83	29.93	11.59	12.23	45.34	29.09	9.57
MDD	6.36	19.65	11.94	2.36	6.36	19.65	11.52	2.33	9.32	18.89	12.91	2.14
OMC	25.76	42.45	32.61	3.61	25.76	42.45	32.52	3.66	27.73	41.69	32.80	3.49
UCS	51.12	527.37	155.75	87.30	51.12	527.37	160.02	93.26	68.55	288.11	145.96	70.84

Min: Minimum, *Max*: maximum, *SD*: standard deviation

The developed ANN model has an MSE value of 0.0001421 and a coefficient of determination value of 0.99990. These final outcomes are achieved after numerous training iterative attempts in which the amount of hidden neurons in the hidden layer and other network variables such as objective, epochs, and learning rate are varied. The network's efficiency is assessed by the amount of mistakes collected in the projected values. The best-trained model is the one that produces the fewest errors. Training is done for 1000 epochs, which implies the network can iterate for a maximum of 1000 rounds to ensure the model's appropriateness. The training has been stopped at the 461^{th} epoch. Fig. 4 and Fig. 5 provide network training state illustrations as well as efficiency graphs, respectively. Table 5 depicts training parameters used in developing a ANN model. Fig. 6 illustrates the regression plot of the projected UCS (Y) of ANN model versus experimental UCS (T) of training data.

Table 5
Training parameters used in a ANN model.

Sl.No.	Neural network characteristics	MATLAB variables and designations
1.	Train function	'trainlm' (levenberg-Marquardt)
2.	Transfer function	'tansig' (no linear function)
3.	Performance function	'mse' (mean square error)
4.	Error after learning	0.001
5.	Train epochs	1000
6.	Input layer neurons count	07
7.	Number of hidden layers	01
8.	Number of neurons in the hidden layer	07
9.	Number of output layer	01
10.	Final architecture	7-7-1

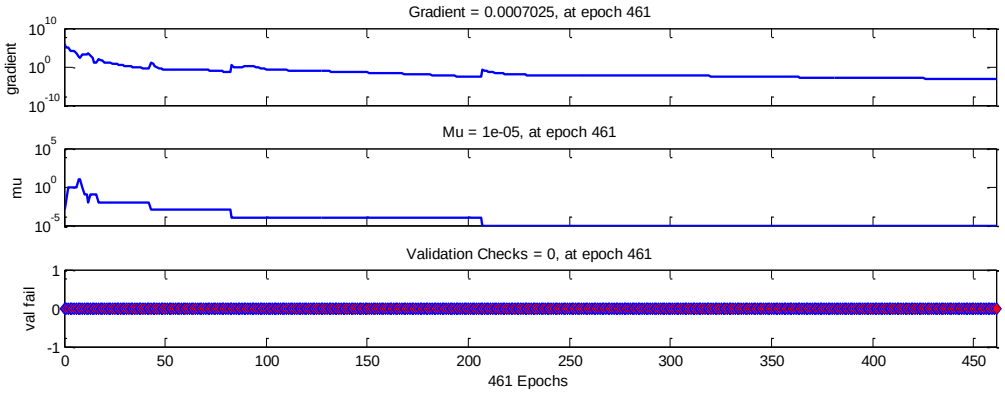

Fig. 4. Network training state illustration.

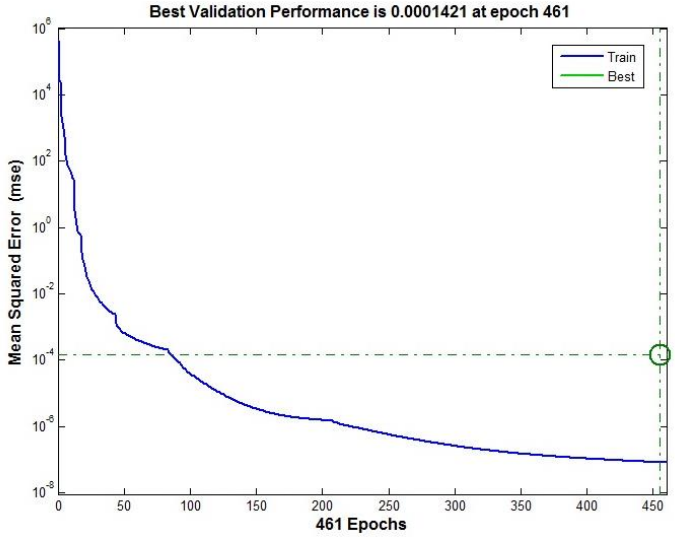

Fig. 5. Plot illustrating training network efficiency.

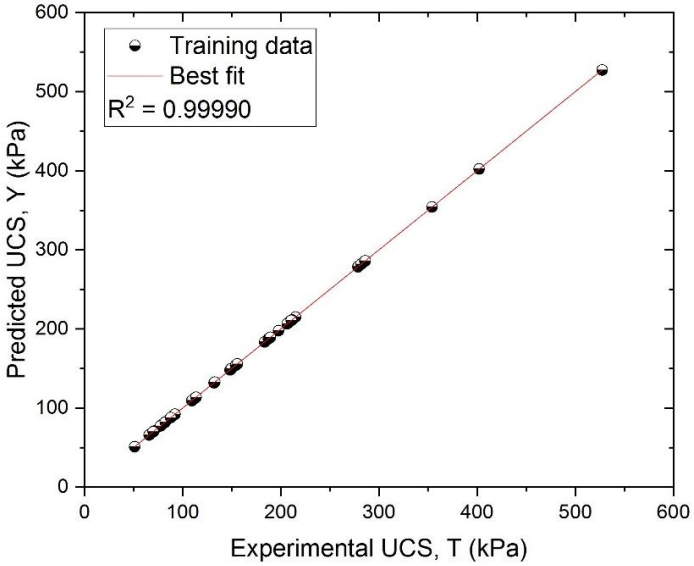

Fig. 6. Regression plot comparing the training data set of ANN model's projected UCS against the experimental UCS.

2.2.1. Testing and validating the trained model

Fig. 7 illustrates the regression plot of the projected UCS (Y) of ANN model versus experimental UCS (T) of testing data. Table 6 provides an overview of the statistical performance of the created ANN model. When using training and testing data, the MAE, RMSE, and R^2 values of the ANN model were 0.0042, 0.0217, and 0.99990 & 0.0038, 0.0104, and 0.99999 respectively. The best-fitting line showed excellent agreement with the line of equality when $R^2 = 0.99990$. As seen in Fig. 6, nearly all of the data points are located comfortably inside the 99% confidence interval range.

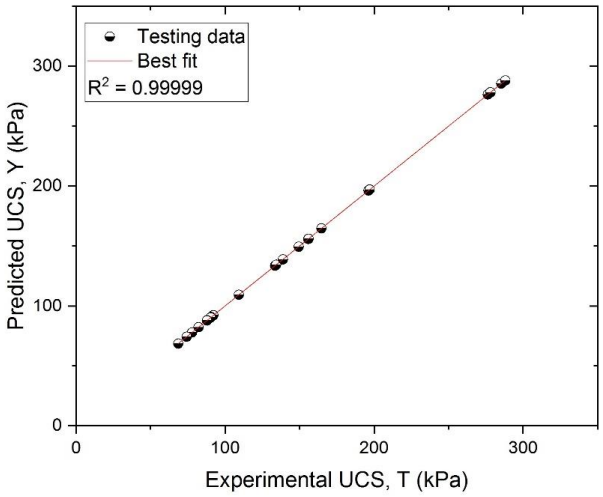

Fig. 7. Regression plot comparing the testing data set of ANN model's projected UCS against the experimental UCS.

Table 6
Efficacy of ANN model.

Model Name	Group of data	Statistical framework		
		R^2	MAE	RMSE
ANN	Training	0.99990	0.0042	0.0217
	Testing	0.99999	0.0038	0.0104

2.3. MVR model development

In the current study, a multi-variable regression analysis (MVR) was also performed to forecast the UCS of soil stabilized using BA-lime. The MVR model was created using 70% of the entire dataset, just like the ANN model. The remaining 30% of the records were used to evaluate the model's predictive capability. The dependent variable and independent variables have a generalized linear relationship that appears as follows:

$$Y = a_0 + a_1X_1 + a_2X_2 + \ldots\ldots\ldots\ldots\ldots + a_pX_p \pm e \quad (4)$$

Where, a_0 is the Y intercept and Y is the dependent variable. The slopes connected to X_1, X_2, and X_p are a_1, a_2, and a_p. e is the error, while X_1, X_2, and X_p are the results of the independent elements. Through the use of least square error optimization, $"a"$ values are generated. UCS was

used as the dependent variable in the MVR model, whereas BA, lime, LL, PL, SL, MDD, and OMC were used as the independent elements.

Table 7
ANOVA of MVR model.

Origin	Degrees of freedom	Sum square	Mean square	F	P
Regression	7	447781.7876	63968.8268	98.11023853	7.38729E-26
Residual	47	30644.45571	652.0096961		
Total	54	478426.2433			

Table 8
Statistical evidence on MVR model predictor variables.

Determinant variable	Coefficients	Standard Error	t-Stat	P-value	Lower 95%	Upper 95%
Intercept	1946.4	323.76	6.012	0	1295.08	2597.72
BA	8.2	4.186	1.959	0.056	-0.221	16.621
Lime	-0.28	3.821	-0.07	0.942	-7.967	7.406
LL	-19.186	5.603	-3.42	0.001	-30.458	-7.914
PL	10.441	2.721	3.837	0	4.966	15.916
SL	16.49	3.01	5.478	0	10.434	22.546
MDD	77.745	8.354	9.306	0	60.938	94.551
OMC	-80.067	7.127	-11.2	0	-94.405	-65.73

Fig. 8 depicts the regression plot of the MVR model for the training data sets of UCS. Table 7 and Table 8 exhibit the outcomes of the analysis of variance (ANOVA) and statistical data for the MVR model's predictor variables. The *F*-test and *t*-test were used to interpret the regression analysis data in Table 7 and Table 8 at a 95% confidence level. Table 7 shows that the *P* value (7.38729E-26) is exceptionally low, indicating that at least one of the MVR model coefficients is significant with a level of confidence (1 - *P*) of almost 100%. However, this F-test is insufficient to identify the crucial MVR model coefficients. Consequently, t-tests were additionally performed to ascertain the significance of particular coefficients. Individual coefficients, *t*-stats, and *P* values are shown in Table 8. The *P* values for the coefficients of the BA, and lime are observed to correlate to rather low levels of confidence (1 - P < 0.95), and they are not remarkable for the model MVR. The *P* value for the LL, PL, SL, MDD and OMC, on the other hand, is relatively low with a strong confidence level (1 - P > 0.95) and indicate that these coefficients are important for the MVR model. The lower and higher limits of the 95% confidence range are also shown in Table 8. The insignificance discovered via *t*-tests of these parameters is compatible with the fact that zero falls within this interval of lime, LL, and OMC with a 95% likelihood of occurring. Since the BA, PL, SL and MDD confidence intervals exclude zero, they agree with the impact of the *t*-tests. Evidently, the MVR model disregarded the importance of lime, LL, and OMC in UCS prediction, which prevented it from generalizing the BA-lime stabilization process in ES.

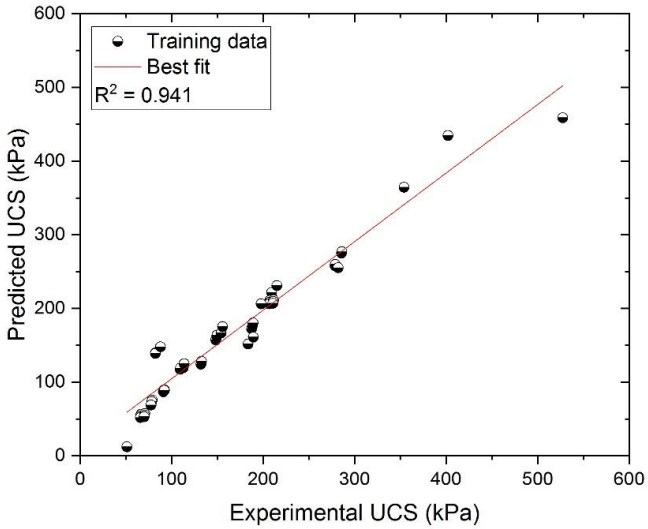

Fig. 8. Regression plot illustrating the variation of training data set of the MVR model.

Table 9
Efficacy of MVR model.

Model Name	Group of data	Statistical framework		
		R^2	MAE	RMSE
MVR	Training	0.941	14.4807	23.6045
	Testing	0.634	25.9416	57.3218

Fig. 9 depicts the regression plot of the MVR model for the testing data sets of UCS. Table 9 provides an overview of the statistical performance of the created MVR model. When using training and testing data, the MAE, RMSE, and R^2 values of the MVR model were 14.4807, 23.6045, and 0.941 & 25.9416, 57.3218, and 0.634 respectively. The statistical results in Table 6 and Table 9 indicate that the ANN model learned and forecasted the experimental data far better than the MVR model.

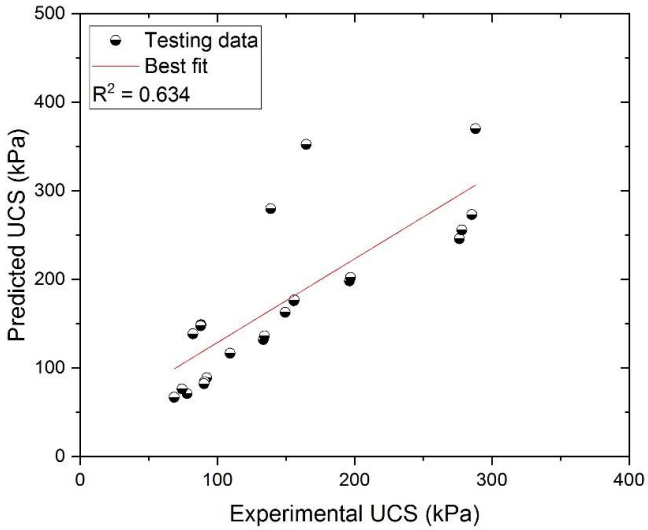

Fig. 9. Regression plot illustrating the variation of testing data set of the MVR model.

2.4. Sensitivity analysis

A sensitivity analysis is carried out to ascertain how delicate a model is to a change in the model's parameter values. Sensitivity evaluation is performed by changing the value of an input variable and observing how the ANN model reacts to this change. It can also be used to identify the most effective parameter values for ANN models, and the sensitivity analysis delivers quite consistent outcomes as to which input element affects the model output [29].

For evaluating variable contributions in geotechnical engineering problems, several academics have had success with approaches like Garson's algorithm and the Connection weight technique. The two approaches mentioned above were employed in the current investigation to identify key input variables for UCS prediction [27]. Using the absolute values of connection weights, the Garson's algorithm divides hidden-output connection weights into components related to each input neuron, known as the "Weights" approach, and computed using equation 5 [27]. Using the equation 6, the Connection weight method computes the product of the actual input-hidden and hidden-output synaptic weights among each input neuron and output neuron, and then adds the products for all hidden neurons [30].

$$Input_x = \sum_{Y=A}^{G} \frac{|Hidden_{XY}|}{\sum_{Z=1}^{7} |Hidden_{ZY}|} \tag{5}$$

$$Input_x = \sum_{Y=A}^{G} Hidden_{XY} \tag{6}$$

In the equations 5 & 6, the weights connecting each input neuron Z (where Z = 1 - 7) to each hidden neuron Y (where Y = A - G) to the single output neuron are used to calculate the variable relevance for predictor variable X (where X = 1 - 7).

3. Results and discussion

3.1. Validation of ANN model

The acquired findings are nearly equal to the experiment data, with a maximum error of 0.0985% in forecasting the UCS values gathered. The mean absolute error (MAE) for the outputs generated with seven hidden neurons was 0.0042. The error histogram is depicted in Fig. 10. The percentage mistakes are classified into 20 groups. Because the error bins are closer to the zero line, it is evident that the constructed ANN model predicts substantial output values within the allowable error margin. As a result, this model can be used for testing and validation. Table 10 shows the comparison of experimental data and ANN outcomes of test datasets.

The absolute percentage errors are likewise within acceptable limits, indicating that the created model predicts outcomes that are similar to the experiment data. In projecting UCS, the greatest absolute percentage error of the test dataset is 0.0348% and the MAE is 0.0038. Fig. 11 depicts a graphical illustration of differences in the UCS's ANN projected outputs, along with experiment data.

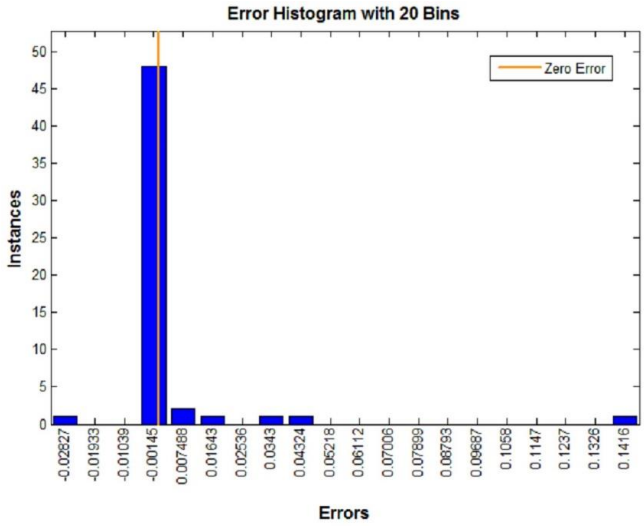

Fig. 10. Error histogram for training data sets of ANN model.

Table 10
Comparison of experimental data and ANN outcomes of test datasets.

Sample No.	Exp.	ANN	Percent error	Sample No.	Exp.	ANN	Percent error	Sample No.	Exp.	ANN	Percent error
4	109.25	109.24	0.0016	**30**	276.32	276.34	0.009	**60**	285.36	285.35	2.68E-05
9	92.22	92.21	0.0002	**36**	278.18	278.18	8E-05	**64**	155.85	155.85	4.98E-05
14	77.91	77.91	3E-05	**40**	149.44	149.44	5E-07	**65**	197.01	197.01	0.000373
17	133.54	133.56	0.0178	**45**	82.25	82.24	0.0042	**69**	87.89	87.85	0.034771
19	90.71	90.71	6E-05	**50**	74.25	74.25	6E-05	**70**	156.03	156.03	0.000996
23	134.31	134.33	0.0162	**51**	88.05	88.04	0.0005	**74**	138.84	138.84	1.06E-06
25	90.32	90.32	0.0042	**57**	87.92	87.92	0.0005	**75**	164.65	164.65	3.26E-07
26	68.55	68.54	0.0002	**59**	196.24	196.23	0.0002	**76**	288.11	288.11	2.96E-07

Exp. = Experimental UCS values (kPa)
ANN = Output values forecasted by the established ANN model (kPa)

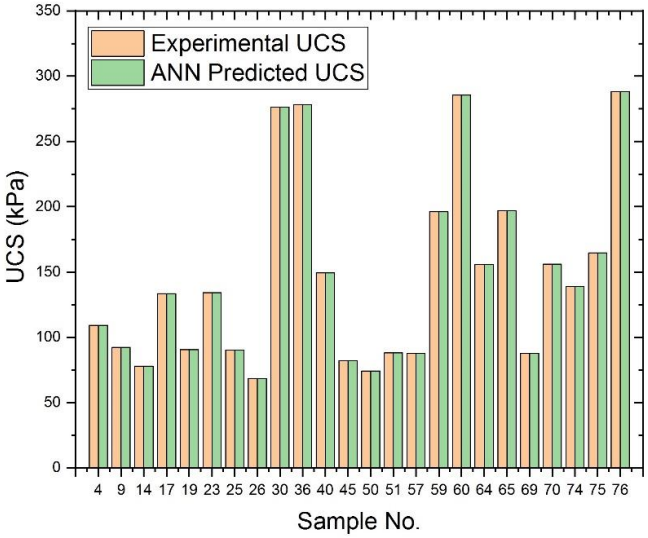

Fig. 11. Variations in UCS of experimental and ANN predicted test output.

3.2. Validation of MVR model

The generated findings are expected to deviate more from the experiment data, with a maximum error of 124.03% in forecasting the UCS values. The mean absolute error (MAE) for the outputs was 14.4807. The error histogram is depicted in Fig. 12. The percentage mistakes are classified into 20 groups.

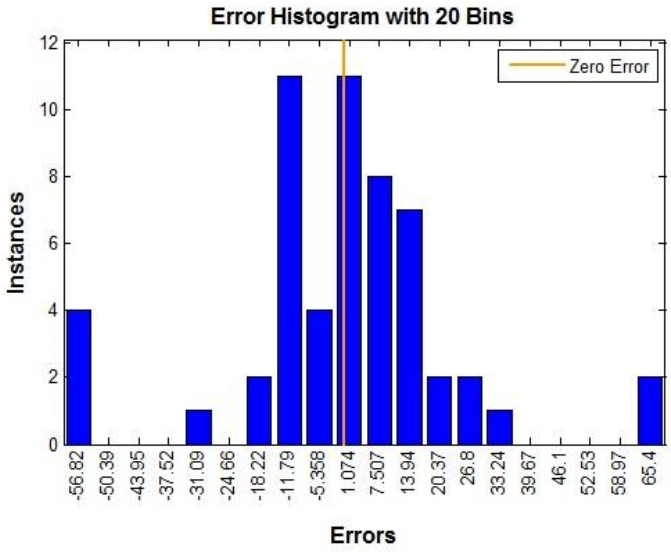

Fig. 12. Error histogram for training data sets of MVR model.

Table 11 shows the comparison of experimental data and MVR outcomes in test datasets. In projecting UCS, the greatest absolute percentage error of the test dataset is 114.084% and the MAE is 25.9416. Fig. 13 depicts a graphical illustration of differences in the UCS's MVR projected outputs, along with experiment data.

Table 11
Comparison of experimental data and MVR outcomes of test datasets.

Sample No.	Exp.	MVR	Percent error	Sample No.	Exp.	MVR	Percent error	Sample No.	Exp.	MVR	Percent error
4	109.25	116.76	6.8803	**30**	276.32	245.90	11.0074	**60**	285.36	273.21	4.2548
9	92.22	89.18	3.2963	**36**	278.18	255.84	8.02736	**64**	155.85	176.03	12.949
14	77.91	71.25	8.5449	**40**	149.44	162.83	8.96581	**65**	197.01	202.43	2.7516
17	133.54	132.32	0.9118	**45**	82.25	138.67	68.6052	**69**	87.89	147.69	68.046
19	90.71	84.65	6.6789	**50**	74.25	76.37	2.86498	**70**	156.03	176.86	13.355
23	134.31	136.35	1.5243	**51**	88.05	148.98	69.2039	**74**	138.84	279.88	101.587
25	90.32	82.39	8.7723	**57**	87.92	148.13	68.4930	**75**	164.65	352.49	114.084
26	68.55	67.03	2.2123	**59**	196.24	198.39	1.09859	**76**	288.11	370.16	28.4810

Exp. = Experimental UCS values (kPa)
MVR = Output values forecasted by the established MVR model (kPa)

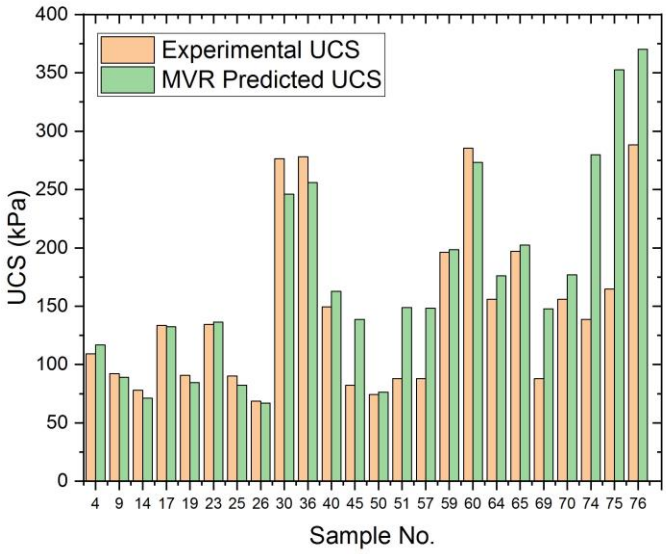

Fig. 13. Variations in UCS of experimental and MVR predicted test output.

From Fig. 13, it is evident that a slight deviation was observed in the MVR predicted values of the UCS for all the test datasets. The primary reason for this kind of behaviour is due to the low coefficient of determination value. This low R^2 states that there is an improper correlation between the input test datasets and the output variable. As seen in Table 8, the MVR model ignored the significance of lime, LL, and OMC in UCS prediction.

3.3. Sensitivity analysis of the developed ANN model

Table 12 displays the ANN model's optimized weight vectors. The significance and relative ordering of various input variables for ANN utilizing Garson's algorithm and the Connection weight approach are displayed in Table 13 focused on the weights referenced there. Table 13 shows that the Garson's algorithm ranked LL as the most crucial parameter and MDD, OMC as the least crucial. Similarly, the Connection weight approach ranked BA as the most important factor while PL represented the minimum effect. Due to the following factors, the ranking provided by the Garson's algorithm appears to be more realistic and acceptable:

a. It is noted that from Table 3 that there has been a gradual increase in the PL value at all dosages of lime content added. This behaviour had reduced the plasticity index (PI) of the soil, giving it better workability. LL is very much essential to calculate the PI of the soil samples. The amount of water that the soil can absorb increases with the plasticity index, increasing the possibility for the soil to swell. Addition of lime to plastic soils, a colloidal reaction occurs that results in an boost in pH, a decrease in double layer water, and the substitution of naturally transported cations on clay surfaces with Ca^{2+} cations. Colloidal clay particles benefit from this by flocculating and aggregating, which lessens their plasticity. Thus, the vital influence was supported by the Garson's algorithm approach's rating of LL and lime as the first and second significant metric.
b. Using the Garson's algorithm approach, SL was evaluated as the third most crucial metric after LL and lime. Because it is observed that raising the BA-lime content leads to an increase in SL and OMC and a slight improvement in MDD. The following causes are

probably what this behaviour is explained by; (1) The effective grading of the soils has been altered by utilizing lime, and this takes place by aggregating the particles to occupy larger spaces; (2) The rise in OMC is the result of a pozzolanic interaction between the soil's clay and the lime; and (3) Typically, lime has a lower specific gravity than the soil sampled.

c. The replacement of BA in the soil mixture, which has a slightly lower specific gravity than soil and requires less compactive energy to achieve its maximum dry density, may be responsible for the little rise in maximum dry density. The interaction between the soil and bagasse ash, which increased the amount of water contained within the flocculent soil structure, and the mixture's higher water absorption due to its lower specific gravity, are likely to contribute to the increase in the ideal moisture content.
d. According to the Garson's algorithm approach, lime is given around 1.468 times as much weight as BA. The UCS of BA-lime treated soil is much greater than that of BA stabilized soil when the mix proportions are same. The interface and interlock processes produced by compactive effort and ageing between clay particles, lime, and BA during the specimen preparation procedure may be responsible for the strength enhancement of BA-lime reinforced ES. The soluble silica and alumina from the clay mineral lattice combine with the calcium available in the lime to form distinct cementitious compounds such as calcium silicate hydrate (CSH) and calcium aluminate hydrate (CAH). With time, these substances solidify, increasing the UCS of the treated ES [6].

Table 12
Weights and biases of ANN model.

Hidden neuron (Y)	A	B	C	D	E	F	G
Weights							
BA	-0.39404	-0.00284	2.5874	-3.6785	-3.599	0.21373	1.1634
Lime	-0.38654	-3.7217	-1.1478	-1.0337	-0.23687	-0.15505	-2.3591
LL	-1.2529	-0.00321	-3.6621	0.99741	2.5453	6.4437	-6.6128
PL	-0.47651	0.002434	-0.73247	4.7897	-1.963	0.58269	-1.9006
SL	-2.9763	-0.00862	-3.246	0.69714	-1.6784	0.63773	2.4178
MDD	-2.2853	-0.04467	0.26626	1.2923	1.3491	-1.2334	0.79001
OMC	-0.24885	0.004418	-0.58344	-0.92545	-0.0437	-0.5026	0.92488
Biases							
Hidden layer	0.45261	3.7014	0.17984	-2.4984	1.0179	-1.5345	-0.42015
Output layer	0.80523						

Table 13
Results of the sensitivity analysis.

Name of a model variable		BA	Lime	LL	PL	SL	MDD	OMC
Garson's algorithm	Importance	0.94	1.38	1.82	0.82	1.05	0.70	0.26
	Relative ranking	4	2	1	5	3	6	7
Connection weight technique	Importance	4.98	-10.58	-8.24	-14.39	-7.40	-1.44	2.44
	Relative ranking	1	6	5	7	4	3	2

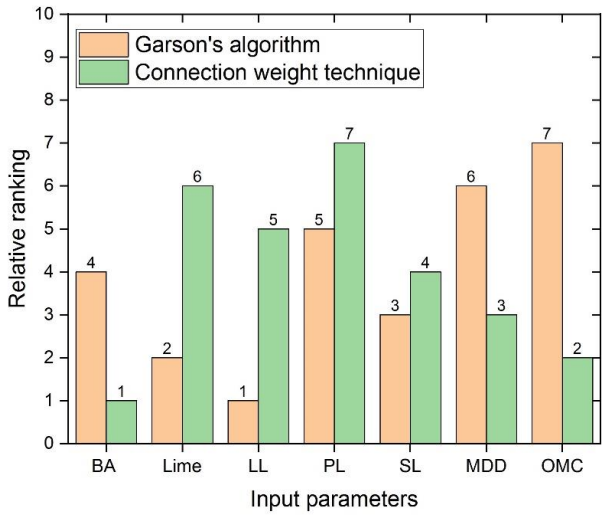

Fig. 14. Plot showing the comparison of Garson's algorithm and Connection weight technique.

Fig. 14 illustrates the comparison of both methods used to identify the importance of input variables in predicting and developing a reliable ANN model.

4. Conclusions

The potential of an artificial intelligence model and multi-variable regression model to forecast the unconfined compressive strength of BA-lime stabilized expansive soil was investigated in this research. From the present study, the following conclusions are drawn:

1. Under equal mix proportions, BA-lime stabilized samples have significantly higher strengths than BA-based stabilized samples, making it is an efficient treatment option for expanding soil.
2. The seven-node ANN model with one hidden layer demonstrates a reliable way to predict the UCS. Using BA, lime, LL, PL, SL, MDD, and OMC as input elements, in computing the 28-day UCS of BA-lime stabilized expansive soil, the ANN model with MLP feed-forward network and back propagation training technique performed better than the MVR model. The value of R^2 acquired by MATLAB programme was 0.99990 for training and 0.99999 for testing, indicating that the ANN has an acceptable assessment capability to estimate the output UCS.
3. According to the MVR model, the important parameters for UCS prediction are LL, PL, SL, MDD and OMC.
4. In contrast to the Connection weight approach, Garson's technique can determine the input factor's actual significance for UCS prediction. The Garson's technique approach states that LL is the factor that has the greatest impact on the prediction of UCS, followed by lime, SL, BA, PL, MDD and OMC.
5. The flexibility and adaptability of the ANN model in terms of data generation can be credited to its superiority over the MVR model in UCS prediction. Contributed data could be used to enhance this model. In future research, it appears to be highly interesting to compare the performance of the existing model and the new model with different activation functions and other learning methods.

References

[1] Javdanian H, Lee S. Evaluating unconfined compressive strength of cohesive soils stabilized with geopolymer: a computational intelligence approach. Eng Comput 2019;35:191–9. https://doi.org/10.1007/s00366-018-0592-8.

[2] Wubshet M, Tadesse S. Stabilization of expansive soil using bagasse ash & lime. Zede J 2014;32:21–6.

[3] Jagadesh P, Ramachandramurthy A, Murugesan R. Overview on properties of sugarcane bagasse ash (SCBA) as Pozzolan. Indian J Geo-Marine Sci 2018;47:1934–1945.

[4] Osinubi KJ, Bafyau V, Eberemu AO. Bagasse Ash Stabilization of Lateritic Soil. Appropr. Technol. Environ. Prot. Dev. World, Dordrecht: Springer Netherlands; n.d., p. 271–80. https://doi.org/10.1007/978-1-4020-9139-1_26.

[5] Nethravathi S, Ramesh HN, Udayashankar BC, Vittal M. Improvement of Strength of Expansive Black Cotton Soil Using Sugarcane Bagasse Ash-Lime as Stabilizer. GeoEdmonton 2018;1:1–6.

[6] Dang LC, Fatahi B, Khabbaz H. Behaviour of Expansive Soils Stabilized with Hydrated Lime and Bagasse Fibres. Procedia Eng 2016;143:658–65. https://doi.org/10.1016/j.proeng.2016.06.093.

[7] James J, Pandian PK. Select geotechnical properties of a lime stabilized expansive soil amended with bagasse ash and coconut shell powder. Sel Sci Pap - J Civ Eng 2018;13:45–60. https://doi.org/10.1515/sspjce-2018-0005.

[8] Srikanth Reddy S, Prasad ACS V, Vamsi Krishna N. Lime-Stabilized Black Cotton Soil and Brick Powder Mixture as Subbase Material. Adv Civ Eng 2018;2018:5834685. https://doi.org/10.1155/2018/5834685.

[9] Goutham DR, Krishnaiah AJ. Improvement in Geotechnical Properties of Expansive Soil Using Various Stabilizers: A Review. Int J Eng Manuf 2020;10:18–27. https://doi.org/10.5815/ijem.2020.05.02.

[10] Ramesh HN, Rakesh C. Influence of Lime Sludge and Sodium Salts on the Strength and Structural Behavior of Clayey Soils–Granite Stone Slurry Dust Composite with Curing. Indian Geotech J 2020;50:801–9. https://doi.org/10.1007/s40098-019-00404-3.

[11] James J, Pandian PK. Bagasse Ash as an Auxiliary Additive to Lime Stabilization of an Expansive Soil: Strength and Microstructural Investigation. Adv Civ Eng 2018;2018:9658639. https://doi.org/10.1155/2018/9658639.

[12] Hossein Alavi A, Hossein Gandomi A, Mollahassani A, Akbar Heshmati A, Rashed A. Modeling of maximum dry density and optimum moisture content of stabilized soil using artificial neural networks. J Plant Nutr Soil Sci 2010;173:368–79. https://doi.org/10.1002/jpln.200800233.

[13] Mozumder RA, Laskar AI. Prediction of unconfined compressive strength of geopolymer stabilized clayey soil using Artificial Neural Network. Comput Geotech 2015;69:291–300. https://doi.org/10.1016/j.compgeo.2015.05.021.

[14] Bunyamin SA, Ijimdiya TS, Eberemu AO, Osinubi KJ. Artificial Neural Networks Prediction of Compaction Characteristics of Black Cotton Soil Stabilized with Cement Kiln Dust. J Soft Comput Civ Eng 2018;2:50–71. https://doi.org/10.22115/scce.2018.128634.1059.

[15] Taleb Bahmed I, Harichane K, Ghrici M, Boukhatem B, Rebouh R, Gadouri H. Prediction of geotechnical properties of clayey soils stabilised with lime using artificial neural networks (ANNs). Int J Geotech Eng 2019;13:191–203. https://doi.org/10.1080/19386362.2017.1329966.

[16] Nazeer S, Dutta RK. Application of Machine Learning Techniques in Predicting the Bearing Capacity of E-shaped Footing on Layered Sand. J Soft Comput Civ Eng 2021;5:74–89. https://doi.org/10.22115/scce.2021.303113.1360.

[17] Dutta RK, Singh A, Gnananandarao T. Prediction of Free Swell Index for the Expansive Soil Using Artificial Neural Networks. J Soft Comput Civ Eng 2019;3:47–62. https://doi.org/10.22115/scce.2018.135575.1071.

[18] Goutham DR, Krishnaiah AJ. Application of Artificial Neural Networking Technique to Predict the Geotechnical Aspects of Expansive Soil: A Review. Int J Eng Manuf 2021;11:48–53. https://doi.org/10.5815/ijem.2021.06.05.

[19] Salahudeen AB, Sadeeq JA, Badamasi A, Onyelowe KC. Prediction of unconfined compressive strength of treated expansive clay using back-propagation artificial neural networks. Niger J Eng 2020;27:45–58.

[20] IS: 2720-Part 4 Methods of Test for Soils: Grain Size Analysis. Bureau of Indian Standards New Delhi. 1985.

[21] IS:1498 Classification and identification of soils for general engineering purposes. Bureau of Indian Standards New Delhi. 2007.

[22] ASTM D 653-03 Standard Specification for Coal Fly Ash and Raw or Calcined Natural Pozzolan for Use. Annual Book of ASTM Standards. 2010:3–6.

[23] IS: 2720-Part 5 Method of testing aggregates. Bureau of Indian Standards New Delhi. 1985:1–16.

[24] IS: 2720-Part VI Determination of shrinkage factors. Bureau of Indian Standard Code New Delhi. 1972:1–12.

[25] IS: 2720-Part VII Determination of water content dry density relation using light compaction. Bureau of Indian Standard Code New Delhi. 1980:1–16.

[26] IS: 2720-Part 10 Determination of unconfined compressive strength. Bureau of Indian Standards New Delhi. 1991:1–6.

[27] Olden JD, Joy MK, Death RG. An accurate comparison of methods for quantifying variable importance in artificial neural networks using simulated data. Ecol Modell 2004;178:389–97. https://doi.org/10.1016/j.ecolmodel.2004.03.013.

[28] Shahin MA, Jaksa MB, Maier HR. Recent Advances and Future Challenges for Artificial Neural Systems in Geotechnical Engineering Applications. Adv Artif Neural Syst 2009;2009:1–9. https://doi.org/10.1155/2009/308239.

[29] Hanandeh S, Ardah A, Abu-Farsakh M. Using artificial neural network and genetics algorithm to estimate the resilient modulus for stabilized subgrade and propose new empirical formula. Transp Geotech 2020;24:100358. https://doi.org/10.1016/j.trgeo.2020.100358.

[30] Valdivia S, Morales A. Determinants of the index of prices and quotations on the Mexican stock exchange: Sensitivity analysis based on artificial neural networks. Glob J Bus Res 2016;10:27–32.